



# Chain-End Functional di-Sorbitan Oleate Monomer Obtained from Renewable Resources as Precursors for Bio-Based Polyurethanes

Susana Valencia-Bermudez<sup>1</sup> · Susana Hernández-López<sup>1</sup> · Manuel Gutiérrez-Nava<sup>2</sup> · José-Manuel Rojas-García<sup>2</sup> · Luis-Edmundo Lugo-Uribe<sup>2</sup>

© Springer Science+Business Media, LLC, part of Springer Nature 2020

## Abstract

A three-step synthetic route was proposed and tested to obtain a chain-end functional di-sorbitan oleate monomer: First, 1,18-octadec-9-enedioic acid compound was produced by self-metathesis reaction of an oleic acid; then, the 1,18-octadec-9-enoyl dichloride compound was yielded by chlorination of the di-acid with thionyl chloride, and finally, the 1,18-di-sorbitan oleate monomer was yielded by esterification of the dichloride with 1,4-sorbitan. The di-sorbitan oleate monomer was purified and then characterized by FTIR, <sup>1</sup>H-NMR, DSC and TGA to establish its structure and properties. A bio-based polyurethane (PU) was synthesized by reacting the obtained 1,18-di-sorbitan oleate monomer and MDI. Rheological analysis showed that a curing reaction occurs as a significant increase of the storage modulus ( $G'$ ) and the complex viscosity ( $\eta^*$ ) at 100 °C. The obtained bio-based PU was characterized by FTIR, TGA and DMA, confirming that 1,18-di-sorbitan oleate is a feasible monomer for synthesizing polyurethanes.

**Keywords** Bio-based polymer · Metathesis · Sorbitan · Polyurethane

## Introduction

In recent years, it has been more relevant to have environmentally friendly alternatives for the development of novel polymeric materials. The main green principles of polymer production include low carbon footprints, high resource effectiveness, clean and lean manufacturing processes, avoid the use of auxiliary substances such as organic solvents and risks to health and the environment, product life cycles controlled with effective waste recycling, and use of renewable feedstocks [1]. This last principle includes all efforts to produce polymers from renewable and bio-based feedstocks

such as: vegetable oils, terpenes, lignin, cellulose, starch, among others.

In addition, alternative strategies have been proposed towards renewable and useful polymers in a green economy, such as: (i) Biomass biorefining and chemical conversion of greenhouse gases into sustainable monomers (ii) bio-based polymers and monomers through the use of living organisms in photobioreactors and (iii) polymers synthesized from carbon dioxide [1]. Bio-refinery represents an emerging industrial system that separates and converts biomass into a range of useful bioenergies and bioproducts, such as biopharmaceuticals, biocosmetics, biochemicals, biomaterials and biofuels. These bio-based products can be classified according to their added-value and volume. Therefore, biopharmaceuticals and biocosmetics products have the highest added-value and biofuels have the highest volume. Biomaterials and biochemicals as feedstocks for producing biopolymers are at a midpoint, with an adequate balance between added value and volume [2]. It is important to keep in mind that efforts are aimed at reevaluating residual biomass without affecting food products [3, 4]. On the other hand, there are some comprehensive reviews on recent developments in macromolecular materials derived from vegetable oil-based monomers, microbially produced monomers and

**Electronic supplementary material** The online version of this article (<https://doi.org/10.1007/s10924-020-01692-0>) contains supplementary material, which is available to authorized users.

✉ Luis-Edmundo Lugo-Uribe  
luisedmundolugo@gmail.com

<sup>1</sup> UAEMEX, Universidad Autónoma del Estado de México, Carretera Toluca - Atlacomulco Km. 14.5, San Cayetano de Morelos, Toluca de Lerdo Edo 50200, México

<sup>2</sup> CIATEQ, A.C, Centro de Tecnología Avanzada, Circuito de la Industria Pte Lte, 11 Mza 3 No 11, Parque Industrial Ex Hacienda Doña Rosa, de México, Lerma Edo 52004, México

polymers, terpenes, lignin, cellulose, chitin and chitosan, starch, urushiol and cardanol monomers, and lactic and lactide polymers, which highlight the importance that this topic has achieved in current years [5–8].

Sorbitol is a sugar alcohol produced from cellulose-based chemical platform, which can be converted into several molecules such as isosorbide, ethanol, lactic acid, glycerol, glycols and sorbitan [9]. Sorbitol dehydration have been studied using different catalytic systems to improve selectivity in the production of isosorbide due to its versatile applications in medicine or pharmaceutical [10–17].

Furthermore, sorbitol has been reported as a biobased monomer to produce a novel polyester using the enzymatic polycondensation process [18]. On the other hand, it has been shown that isosorbide is a relevant compound for preparing biopolymers such as polyesters, polycarbonates, polyurethanes and epoxy resins, particularly for replacing bisphenol A in polycarbonate production and improving the properties of poly(ethylene terephthalate) (PET) [10, 19, 20]. Nevertheless, there are few reports on the use of 1,4-sorbitan as a precursor to develop bio-based polymers. An example of this application includes the synthesis of sorbitan methacrylate to synthesize hydrogels [21]. The main use of 1,4-sorbitan is to produce emulsifying agents such as sorbitan esters and polysorbates. Thus, this compound has been used in the synthesis of bio-based materials [22, 23].

Novel polyurethanes (PU) reported in the literature were obtained from fatty acid derivatives through different research routes.

A first route considers that the synthesis of plant-derived polyurethanes that have unique properties is possible by reacting fatty acid-based diisocyanates with bio-based polyols [24–26]. Other routes include chemical processes, such as: (1) acyclic triene metathesis polymerization (ATMET) to produce some shape memory polyurethanes [27], (2) enzymatic route to produce soybean oil-based shape memory polyurethanes [28], (3) combination of some glycols derived from different vegetable oil and poly(-caprolactone) diol to yield hyperbranched shape memory polyurethane [29], and (4) one-step synthesis to produce epoxidized rapeseed oil-based polyurethane network [30].

Cross metathesis has been one of the most important chemical routes applied in obtaining new molecules from renewable resources, specifically, compounds derived from biomass or vegetable oil [31–39]. In this study, cross metathesis was used to produce functional chain-end functional di-sorbitan oleate monomer. A three-step synthetic route was proposed and evaluated to produce a di-sorbitan monomer and use it in the synthesis of bio-based polyurethanes. According to the state of the art, this study presents for the first time a vegetable oil-based monomer that contains 1,4-sorbitan groups at both ends of its structure and that has been tested in the synthesis of polyurethanes.

## Experimental

### Materials

Second generation Grubbs catalyst, oleic acid (90% purity), Dimethylethanolamine ( $\geq 98\%$  purity), D-sorbitol 99%, Thionyl chloride ( $\geq 99\%$  purity), triethylamine ( $\geq 99.5\%$  purity),  $1 \mu\text{mol H}_2\text{SO}_4$  aqueous solution, hexane (95% purity), dichloromethane (99.8% purity), dichloroethane ( $\geq 99\%$  purity), ethyl acetate (99.8% purity), methanol ( $\geq 99.9\%$  purity), cis-2-butene-1,4-diol (97% purity) and tetrahydrofuran were purchased from Sigma-Aldrich. Diphenylmethane 4,4'-diisocyanate (mixture of di and triisocyanates, melting temperature  $10^\circ\text{C}$ ) was purchased from Merck. Resin for size exclusion chromatography (SEC SX-1) was purchased from Biorad.

1,18-octadecenediol was produced by metathesis reaction of oleyl alcohol according to a method described in previous work [40].

### Synthesis of 1,18-Octadec-9-enedioic Acid

1,18-octadec-9-enedioic acid was synthesized as shown in Fig. 1a according to the method described by Ngo et al. [35, 36].

For the reaction, 200 mL (0.633 mol) of oleic acid and 0.244 g ( $2.8 \times 10^{-4}$  mol) of second generation Grubbs catalyst (previously dissolved in 10 mL of dichloromethane) were mixed in a 500 mL Schlenk flask. The mixture was maintained for 48 h at  $55^\circ\text{C}$ , under a nitrogen atmosphere and constant stirring, and then, quenched with 0.013 mL of dimethylethanolamine (DMEA).

The product 1,18-octadec-9-enedioic acid was purified by column chromatography using a hexane / ethyl acetate mixture (95/5 v:v), where the by-product, 9-octadecene was separated.

### Dehydration of Sorbitol

The dehydration reaction of D-sorbitol was carried out following the procedure described by Yabushita [41, 42]. The reaction was carried out in a three-neck flask in which a condenser and vacuum system was placed to continuously remove the produced water. 4 g (0.022 mol) of sorbitol and 0.5 mL of  $1 \mu\text{mol H}_2\text{SO}_4$  aqueous solution were loaded into the three-neck flask. Then, the reaction was performed at  $130^\circ\text{C}$  under constant stirring for 120 min.

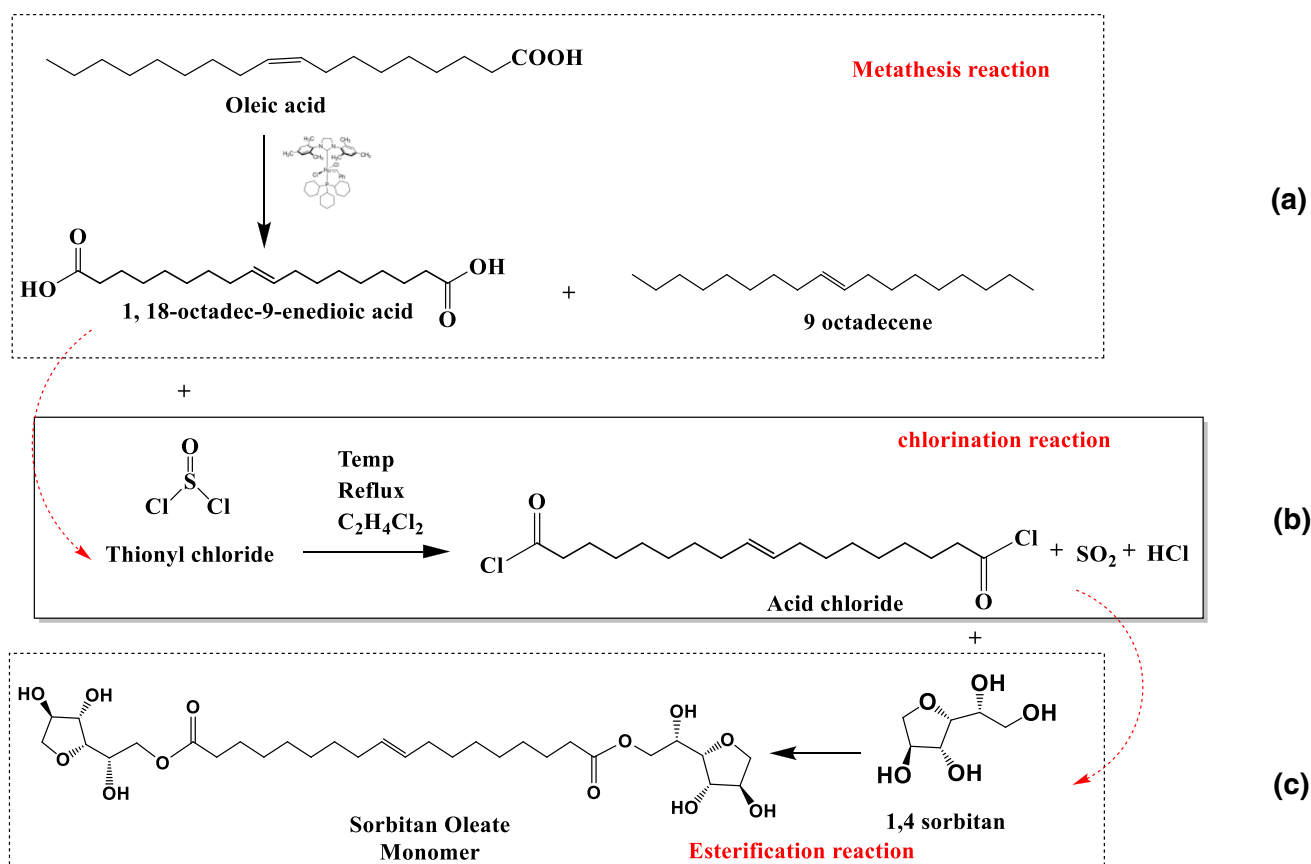


Fig. 1 Synthesis route to obtain chain-end di-sorbitan oleate monomer

### Chlorination Reaction

The reaction scheme is shown in Fig. 1b. 5 g (0.016 mol) of 1,18-octadec-9-enedioic acid, 40 mL of dichloroethane and 2.5 mL (0.034 mol) of thionyl chloride (SOCl<sub>2</sub>) were added in a ball flask. The chlorination reaction was carried out at 80 °C under constant stirring and reflux. The reaction was monitored with infrared spectroscopy. The remaining dichloroethane was removed by rotary evaporation, taking care that the rotavapor is free of moisture; otherwise, the product could return to the carboxylic acid form. If the esterification reaction is not carried out immediately, the material must be kept under vacuum to avoid possible contamination of the product with moisture.

### Esterification Reaction

The esterification reaction scheme is presented in Fig. 1c which was carried out with 5.3 g (0.032 mol) of 1,4 sorbitan dissolved in 60 mL of dichloroethane and 1.6 g (0.016 mol) of acid chloride by using a reaction system consisting of a ball flask placed on a heating plate, a rotary condenser attached to the flask to maintain solvent reflux and a

moisture trap placed at the condenser outlet. The esterification reaction was carried out at 80 °C for 60 min with magnetic stirring. Then, 2.5 mL (0.018 mol) of triethylamine was added dropwise. The residence time was approximately two more hours. The reaction progress was monitored by IR spectroscopy. At the end of the reaction, the remaining solvent was distilled off and the main product was purified.

### Monomer Purification

The monomer purification was made by two-step process: purification by size exclusion and polarity.

(a) Step 1. Size exclusion separation process (SEC).

A separation column prepared with 16.2 g of SEC SX-1 resin and 350 mL of tetrahydrofuran was conditioned for 24 h. For the purification of 3 g of the monomer in the prepared separation column, tetrahydrofuran was used as eluent phase. The fractions were collected considering a constant elution volume of 10 mL and the purification was corroborated by infrared spectroscopy.

(b) Step 2. Separation process using polarity difference

In this step, the sorbitan oleate monomer-rich fractions obtained in step 1 (SEC) were separated using dichloromethane as eluent phase in a second separation column prepared with silica. The fractions obtained were evaluated by infrared spectroscopy. The purified monomer was used for the polymerization of the polyurethane.

### Synthesis of Bio-Based Polyurethane

The polymerization was carried out in a stainless-steel mold, which produces a sample with the dimensions required in dynamic mechanical analysis (DMA).

0.744 g of di-sorbitan monomer and 4,4'-diphenylmethane diisocyanate were placed at a 1: 1 molar ratio in the mold, which was heated at 60 °C for 15 min to extract any volatile material. Then, the temperature was increased to 120 °C, and the mold was subjected to 7 tons of compression force, where the material was cured for 30 min. After cooling the mold, the polyurethane was recovered and characterized. Two additional polyurethanes were prepared to compare the behavior of the PU obtained with di-sorbitan oleate monomer. For this, 1,4-butanediol and 1,18 octadecenediol were used to carry out the reaction with MDI at a 1: 1 molar ratio.

### Characterization of 1,4 Sorbitan

The 1,4 sorbitan was characterized by Attenuated Total Reflectance—Fourier transformed infrared spectroscopy (ATR-FTIR), differential scanning calorimetry (DSC), thermogravimetric analysis (TGA) and proton nuclear magnetic resonance (<sup>1</sup>H-NMR) using the same equipments that have been used in the analysis of the monomer and polyurethane. The 1,4 sorbitan was dissolved in H<sub>2</sub>O + TMS to be analyzed by <sup>1</sup>H-NMR. Additionally, the 1,4 sorbitan was analyzed by liquid chromatography using a YL9100 HPLC instrument, the mobile phase was a solution of 0.005 N sulfuric acid at a flow of 0.6 mL/min at 60 °C. The column used was Rezek organic acid (ROA) 300 × 7.8 mm, and the analysis was carried out for 35 min.

### Characterization of Bio-Based Monomer and Polyurethane

Bio-based monomer obtained from cross metathesis of fatty acid derivatives was characterized by ATR-FTIR, DSC, TGA, and <sup>1</sup>H-NMR whereas bio-based polyurethane was characterized by ATR-FTIR, DSC, TGA, oscillatory rheometry and DMA.

ATR-FTIR analysis was made by using a Cary 4500a spectrometer with spherical diamond crystal in 650–4000 cm<sup>-1</sup> range. Thermal transitions were obtained using a TA-Instruments DSC Q2000. Samples were placed

on a hermetic aluminum pan and were analyzed under inert atmosphere. All cycles were performed at a heating rate of 10 °C/min and a temperature range from 20 °C to 150 °C for the monomer and from –90 °C to 150 °C for the polyurethane. The thermogravimetric analysis (TGA) was performed using a TA-Instruments TGA Q50 at a heating rate of 10 °C/min from 40 °C to 600 °C under nitrogen atmosphere and from 600 °C to 900 °C at same heating rate under air atmosphere. <sup>1</sup>H-NMR was performed using a Brüker Avance-III 500 (500 MHz, acetone-d<sub>6</sub>) spectrometer.

The rheological analysis was performed in a TA-Instruments rheometer AR 2000 by using a 25 mm-parallel plate geometry. Temperature sweep experiment was performed from 20 to 130 °C at a heating rate of 3 °C/min, 1.25% strain and 1 Hz frequency.

The dynamic mechanical analysis (DMA) of the synthesized polyurethane was performed in a TA-Instruments DMA Q800, by the following conditions: Film tension mode (16.5 mm × 9.7 mm × 1.35 mm), temperature range from –90 °C to 150 °C at a heating rate of 3 °C/min, 0.5 N preload, 1 Hz oscillation frequency and 10–20 μm amplitude.

## Results and Discussion

### Sorbitol Dehydration to Obtain 1,4-Sorbitan

A homogeneous phase dehydration process described by Yabushita [41] was employed under acidic conditions using H<sub>2</sub>SO<sub>4</sub> as catalyzer to selectively convert sorbitol to 1,4-sorbitan avoiding dehydration up to isosorbide [42]. Then, the obtained 1,4-sorbitan was used in esterification reactions to synthesize di-sorbitan oleic monomer. Several physicochemical analyzes were performed (DSC, TGA, HPLC and <sup>1</sup>H-NMR) to confirm 1,4-sorbitan structure.

DSC thermograms show a melting point (T<sub>m</sub>) at 95 °C for sorbitol and 67 °C for 1,4-sorbitan compound. TGA thermograms show that thermal degradation is observed at 304 °C for 1,4-sorbitan and 319 °C for sorbitol, therefore, a completely separated decomposition temperature (T<sub>d</sub>) is clearly observed. (DSC and TGA thermograms are included as Support Information).

HPLC analysis shows that the retention time for sorbitol is 10.92 min. Chromatogram of the sorbitol dehydration product shows two peaks, one located at 10.94 min attributed to the remaining sorbitol compound and other peak found at 11.44 min relating to 1,4-sorbitan, in agreement with Yabushita et al. [41]. They determined that the retention time for D-sorbitol is 16.6 min, for 1,4-sorbitan is between 17.0 and 18.0 min and for isosorbide is 20.9 min. The slight variation in retention times is due to difference in the selected columns. According to the areas obtained from the

chromatogram, the conversion of the sorbitol dehydration reaction was 72.7% (66% of 1,4-sorbitan, 2.1% of an unidentified sorbitan isomer and 4.6% of isosorbide.). Therefore, it was confirmed that sorbitol dehydration product contains a mixture of unreacted sorbitol and 1,4-sorbitan and a moderate quantity of other compounds (HPLC chromatograms are included as Support Information.).

Figure 2a shows the  $^1\text{H-NMR}$  spectra of the used D-sorbitol and its dehydration product (1,4-sorbitan and other isomers). Peak assignment for protons in sorbitol were made considering literature references [41, 42]:  $\delta$  4.28 (1H, d, H-C<sub>5</sub>);  $\delta$  4.23 (1H, d, H-C<sub>4</sub>);  $\delta$  4.13 (1H, dd, H-C<sub>6</sub>);  $\delta$  3.89 (1H, dd, H-C<sub>3</sub>);  $\delta$  3.86 (1H, ddd, H-C<sub>2</sub>);  $\delta$  3.79 (1H, dd, H-C<sub>1</sub>);  $\delta$  3.71 (1H, d, H-C<sub>6</sub>) and  $\delta$  3.62 (1H, dd, H-C<sub>1</sub>).

Figure 2b shows the  $^1\text{H-NMR}$  spectrum of the obtained 1,4-sorbitan. As can be seen, new chemical shifts are observed at a low field between 4.30 and 4.10 ppm in agreement with Yabushita et al. [41]

Evidence of other peaks attributed to other isomers like isosorbide, 2,5-mannitan or 2,5-iditan were not found by  $^1\text{H-NMR}$ , but from HPLC results we know that around 6% of the product corresponds to some of these isomers. The

signals related to sorbitol may be present in the spectrum of Fig. 2b but overlap the signals corresponding to 1,4-sorbitan (from HPLC, the sample must contain approximately 27% of sorbitol).

### Chlorination and Esterification Reactions

Oleic acid self-metathesis process with 0.1 mol% of a second generation Grubbs catalyzer according with methodology described in previous works [35, 36, 40] was used to synthesize an end-functional di-acid oleic monomer (1,18-octadec-9-enedioic acid). The conversion efficiency was 48.5% (23.8 g produced) determined after separation of solid di-acid from oleic acid with a purity of 98% measured by chemical shifts at 0.9 ppm assigned to residual  $-\text{CH}_3$  protons in  $^1\text{H-NMR}$  spectra.

In order to increase end-terminal functional groups reactivity to facilitate esterification reaction with 1,4-sorbitan, chlorination of 1,18-octadec-9-enedioic acid was carried out through reaction with thionyl chloride in 1,2-dichloroethane at 80 °C. Reaction evolution was followed through ATR-FTIR spectrometry. Figure 3 shows

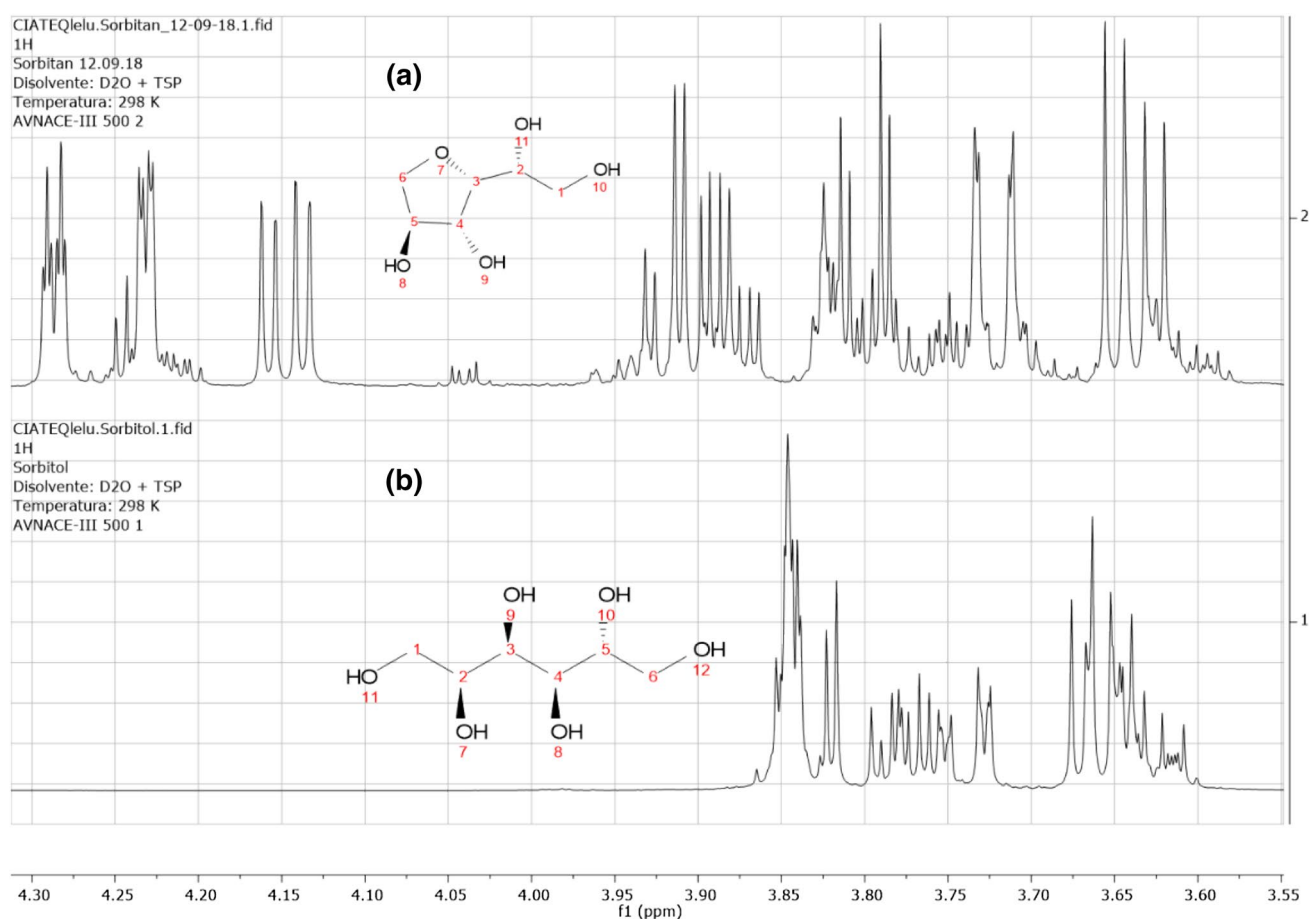


**Fig. 2**  $^1\text{H-NMR}$  spectra comparative of **a** sorbitol and **b** 1,4-sorbitan

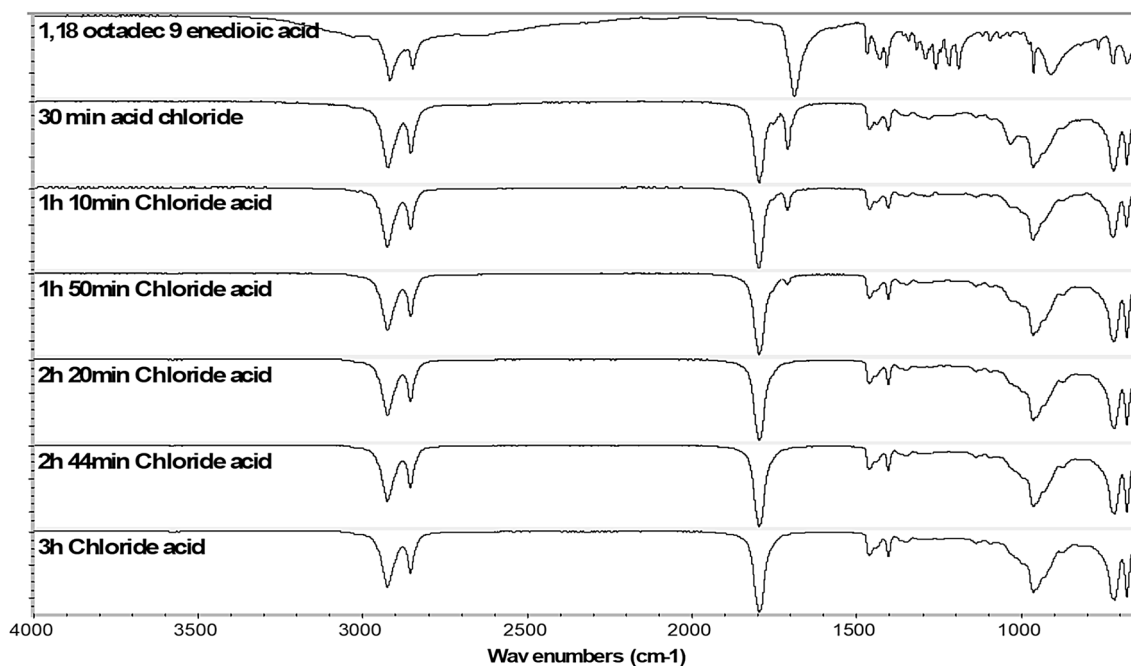


Fig. 3 FTIR spectra for chlorination reaction evolution

FTIR spectra of the product of chlorination of 1,18-octadec-9-enedioic acid at different reaction times. It can be observed between  $2500\text{ cm}^{-1}$  and  $3500\text{ cm}^{-1}$  how stretching vibration signal of the hydroxyl unit of the acid group disappear after one-hour reaction. Also, another change

can be observed at  $1690\text{ cm}^{-1}$  attributed to the carbonyl acid signal; as chlorination reaction takes place, and  $-\text{OH}$  group is changed by  $-\text{Cl}$ , carbonyl signal is displaced to  $1796\text{ cm}^{-1}$ . After 2 h, chlorination reaction is completed, since acid carbonyl has disappeared.

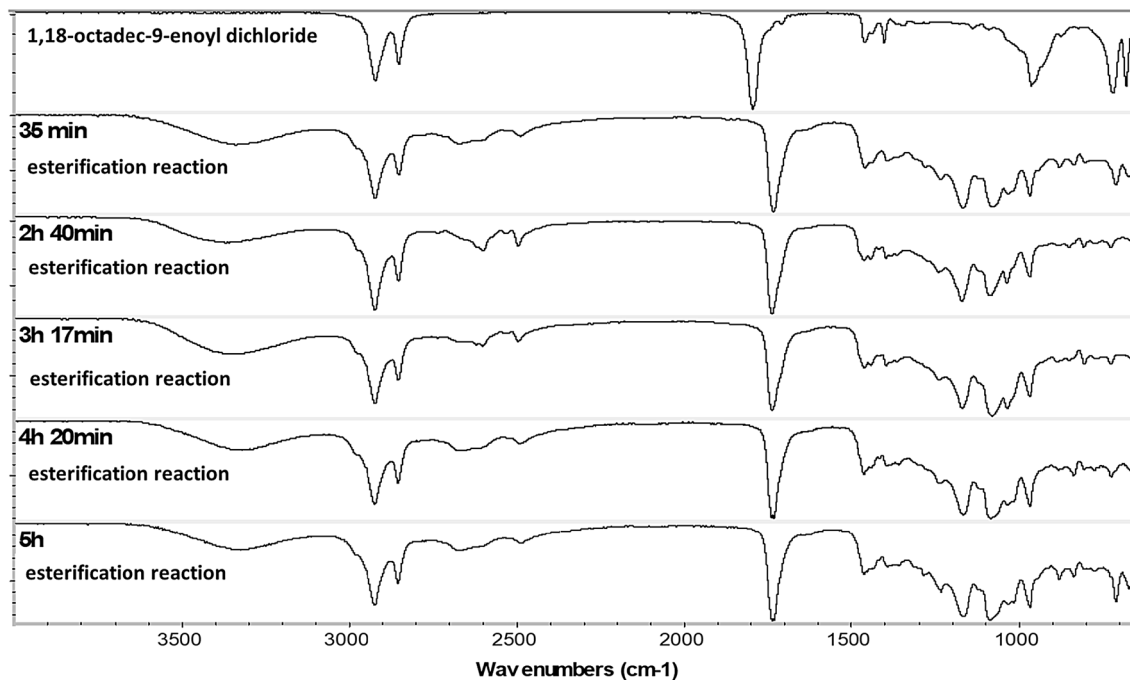


Fig. 4 FTIR spectra for esterification reaction evolution of 1,18-octadec-9-enoyl dichloride with sorbitan



Esterification was carried out reacting 1,18-octadec-9-enoyl dichloride and 1,4-sorbitan in presence of triethylamine to shift the chemical balance to the formation of the ester. Figure 4 presents FTIR spectrum evolution with respect to esterification reaction time. After reacting 35 min, a shift is observed from  $1796\text{ cm}^{-1}$  corresponding to the carbonyl group of the acid chloride to  $1737\text{ cm}^{-1}$  corresponding to carbonyl of the sorbitan ester. As reaction time increases, other signals augment like  $\text{-OH}$  absorption band between  $3200$  to  $3500\text{ cm}^{-1}$  or stretching vibration of  $\text{C-O}$  bonds that can be observed in the region amidst  $1000$  to  $1400\text{ cm}^{-1}$  associated to different  $\text{-OH}$  groups in sorbitan. This kind of  $\text{C-O}$  vibration bands are not observed in spectrum of 1,18-octadec-9-enoyl dichloride, since  $\text{-OH}$  of the acid group was substituted by chloride. On the other hand, trans double bond signal at  $965\text{ cm}^{-1}$  is still present both in the oleic dichloride and in the di-sorbitan oleate, indicating that oleic unsaturation remains intact.

Esterification reaction product was purified by two-steps methodology, one first-step using a size exclusion column (SEC) to eliminate triethylammonium chloride yielded during esterification by reaction between triethylamine and  $\text{HCl}$ , this last compound is a by-product of chloride substitution by sorbitan, and a second-step using polar chromatography with a silica column. After this second-step, purified di-sorbitan oleate monomer was recovered and characterized (only SEC fraction 2 to 6 were used for characterization and evaluation in PU synthesis). The

yield of the esterification reaction after purification was calculated obtaining a value of 85.7%.

Thermal properties of di-sorbitan oleate monomer were measured by DSC and TGA. DSC thermogram shows a melting temperature ( $T_m$ ) at  $15\text{ }^\circ\text{C}$  with a melting enthalpy ( $Q_m$ ) of  $25.4\text{ J/g}$  and its crystallization temperature ( $T_c$ ) at  $0\text{ }^\circ\text{C}$  with a crystallization enthalpy ( $Q_c$ ) of  $30.9\text{ J/g}$ . Thermal stability of the di-sorbitan oleate monomer was established by TGA, observing that its thermal decomposition process begins around  $200\text{ }^\circ\text{C}$  with a decomposition peak ( $T_d$ ) at  $405\text{ }^\circ\text{C}$ . Both DSC and TGA thermograms are included in the support information document.

As seen in Fig. 5, FTIR spectra shown for (a) 1,18-octadec-9-enedioic acid (b) 1,18-octadec-9-enoyl dichloride and (c) 1,18-di-sorbitan oleate monomer are clearly defined both in their characteristic bands and in their functional groups.

The main differences are observed in the carbonyl group: (a)  $\text{COOH} - 1700\text{ cm}^{-1}$ ; (b)  $\text{COCl} - 1796\text{ cm}^{-1}$  and (c)  $\text{COOR} - 1737\text{ cm}^{-1}$ . The presence of hydroxyl groups is critical to ensure reactivity of the oleic di-sorbitan ester, since these functional groups are thought to react with isocyanate group. Both stretching vibration of  $\text{O-H}$  at  $3200$  to  $3500\text{ cm}^{-1}$  and stretching vibration of  $\text{C-O}$  (alcohols) at  $1000$  to  $1400\text{ cm}^{-1}$  are strong signals in the oleic di-sorbitan monomer, suggesting a feasible important reactivity with isocyanate to produce urethane groups.

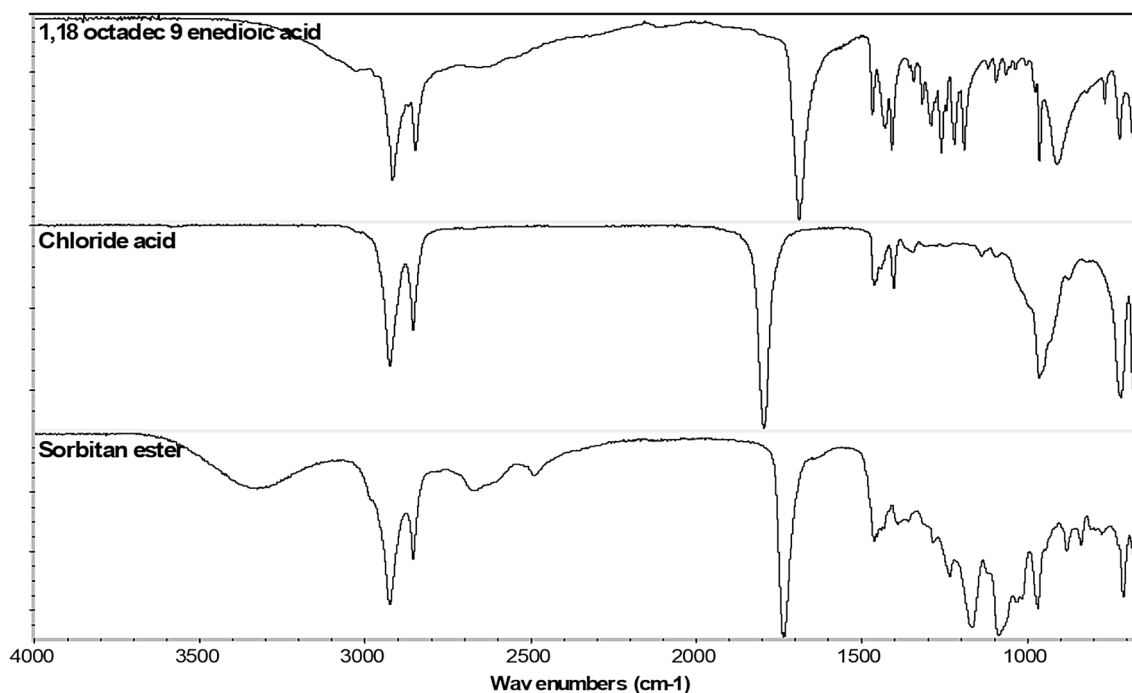
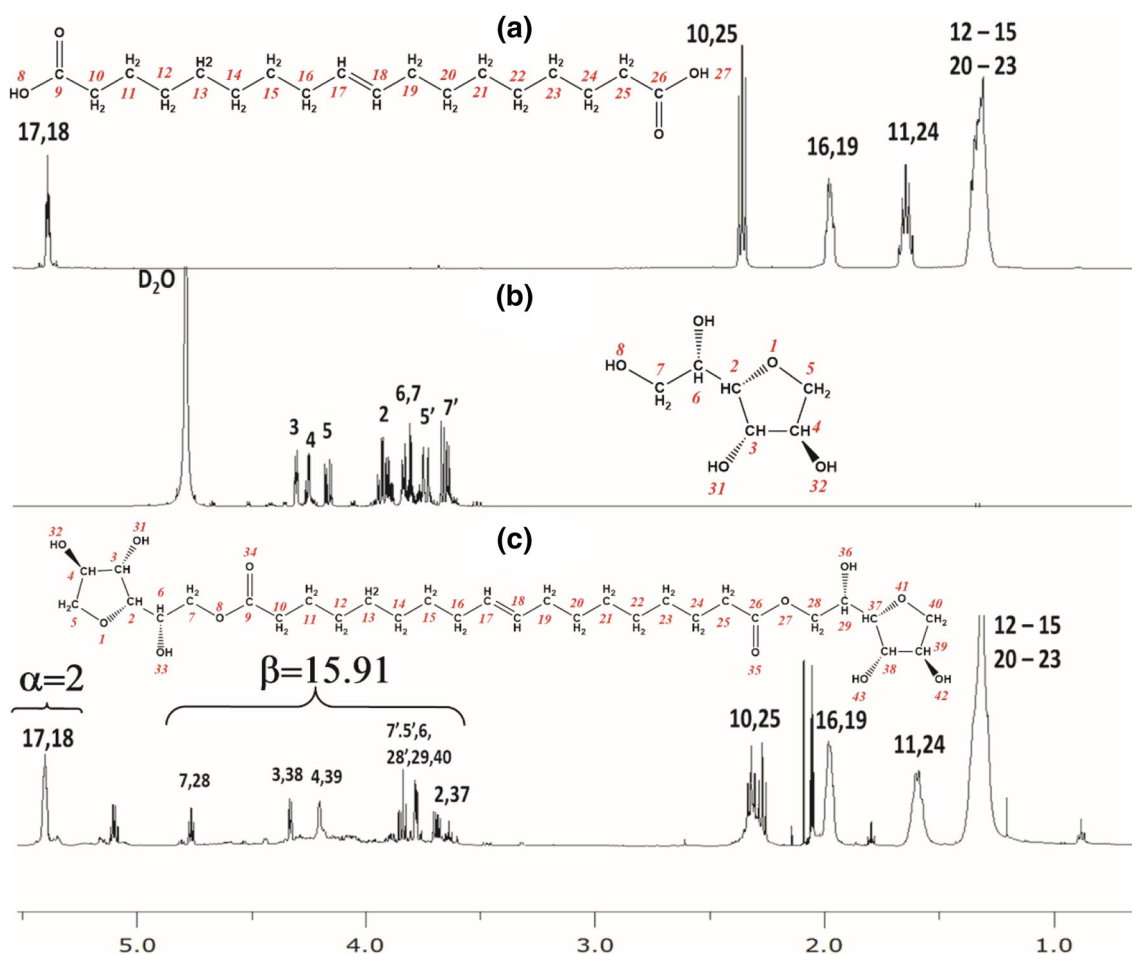


Fig. 5 Comparison of FTIR spectra of a 1,18 octadec-9-enedioic acid b 1,18-octadec-9-enoyl dichloride and c 1,18-di-sorbitan oleate



**Fig. 6**  $^1\text{H-NMR}$  spectra comparative of **a** 1,18-octadec-9-enedioic acid **b** 1,4-sorbitan and **c** 1,18-di-sorbitan oleate

$^1\text{H-NMR}$  spectra of 1,18-octadec-9-enedioic acid, 1,4-sorbitan and 1,18-di-sorbitan oleate are shown in Fig. 6a, b and c respectively. Comparing spectra (a) and (c), aliphatic methylene protons of oleic chain can be observed in both spectra at high field:  $\delta$  1.3 ppm (H12 to H15 and H20 to H23),  $\delta$  1.6 ppm (H11 and H24) and  $\delta$  2.0 ppm (H16 and H19); the same as occurs with methine protons of oleic unsaturation:  $\delta$  5.4 ppm (H17 and H18).

As seen in Fig. 6c, at 2.3 ppm a broader signal attributed to methylene protons of  $\beta$  carbons (protons H10 and H25) was found for the di-sorbitan oleate compound than the corresponding one for the oleic di acid compound because the effect of neighborhood of ester group instead of an acid group in the chemical structure.

Assignations for the  $^1\text{H-NMR}$  spectrum of the 1,18-di-sorbitan oleate corresponding to sorbitan group were made considering the spectrum of 1,4-sorbitan (Fig. 6b) and a simulated spectrum obtained by using MestReNova<sup>TM</sup> software. Most significant change can be observed in protons of methylene bridge (H7 and H28) next to ester group. These same protons in 1,4-sorbitan compound are adjacent to a

hydroxy group instead to an ester, showing chemical shifts close to 3.6 ppm (H7') and 3.8 ppm (H7). After ester group formation, the chemical shifts of these protons change to lower field values: 3.82 ppm (H7') and 4.8 ppm (H7).

In order to determine the addition of sorbitan groups to both ends-chain of the oleate molecule, a ratio obtained was calculated by dividing the area of the signals corresponding to the protons of sorbitan group (area  $\beta = 15.91$ ) and the area of the methine protons of the double bond in the oleic chain ( $\alpha = 2$ ). The integrated  $^1\text{H-NMR}$  spectrum can be consulted in Supporting Information document. This ratio is close to 8, which is in accordance with the number of protons of the sorbitol group (16; without considering the protons of the hydroxy groups that doesn't shown chemical shift in the  $^1\text{H-NMR}$ ) and with the number of protons of the methines of the double bond (2) that should appear in the 1,18-di-sorbitan oleate molecule.

It is important to mention that the evidence we have acquired allows us to deduce that the monomer we obtained mainly contains the structure of 1,18-di-sorbitan-oleate. However, according to the results of each of the reaction



steps, it is likely the final product also contains some structure associated with residual sorbitol and other remaining isomers. This can only be verified by deepening the characterization of the compound through techniques such as mass spectrometry (MS) and carbon magnetic resonance ( $^{13}\text{C}$ -NMR).

## Polyurethane Synthesis

For a long time, vegetable oil derivatives have been used to produce bio-based polyurethanes because in the oil-based triglyceride structures, several functional groups should be present that allow the production of bio-based polyols or even bio-diisocyanates [6, 7, 43–47].

In this study, the effect of 1,4-sorbitan groups at the ends of an oleic monomer chain is elucidated to get multiple hydroxyl functionalities that can react with diisocyanates to produce a controlled cross-linked polyurethane.

A proposed chemical structure that could be formed by the reaction of the 1,18-di-sorbitan oleate monomer with 4,4-methylene diphenyl diisocyanate (MDI) is shown in Fig. 7. In this polymerization reaction, diisocyanate can react with three secondary alcohols: one of them is aliphatic, and two of them are cyclic, allowing to form a network structure.

In most cases, a secondary alcohol is less reactive than a primary alcohol, but in the case of reactions with isocyanate groups, some studies have shown that even secondary cyclic alcohols can be highly reactive to form urethane [48, 49]. On the other hand, there is evidence that sugar alcohols,

like 1,4-sorbitan, exhibit significant reactivity with MDI to produce polyurethanes [50].

The obtained thermo-rheology data allowed to study the polymerization reaction between 1,18-di-sorbitan oleate monomer and MDI. Different molar ratios between these monomers were evaluated to determine the mixture with the highest reactivity for the formation of PU. Figure 8 shows as a function of the temperature, (a) the storage modulus ( $G'$ ) and loss modulus ( $G''$ ), and (b) the complex viscosity ( $\eta^*$ ).

It is possible to establish, through the curves in Fig. 8, the temperature at the gel point, either by means of the crossover between modules  $G'$  and  $G''$  or by a significant change in the slope of the complex viscosity as a function of temperature. Then, for instance, the gel point was established at 110 °C for 1:1 molar ratio. Above this value, both moduli and complex viscosity increase remarkably pointing out that polyurethane formation yields a more elastic molecular structure.

It was expected that molar ratio with higher isocyanate content would work better due to the number of active hydroxy groups presented in the sorbitan group, however, the most encouraging results were obtained with 1:1 molar ratio. This is explained since MDI is a mixture of diisocyanates and triisocyanates that could change the number of available functional groups, in addition to the fact that not all hydroxy groups in the sorbitan can react with an isocyanate.

Curing process of polyurethane with other aliphatic diols is observed in Fig. 9 through following complex viscosity behavior as function of temperature. Polyurethanes synthesis of Butenediol/MDI (■) and 1,18 octadecenediol/MDI (▼) were reported in previous work [40]. Additionally, in the

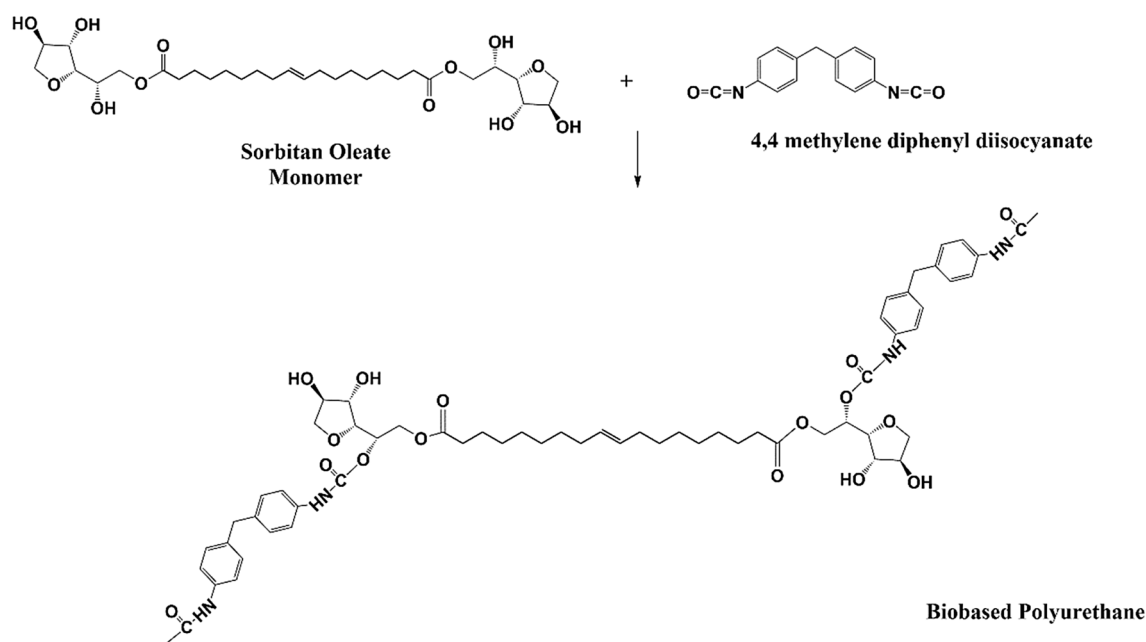
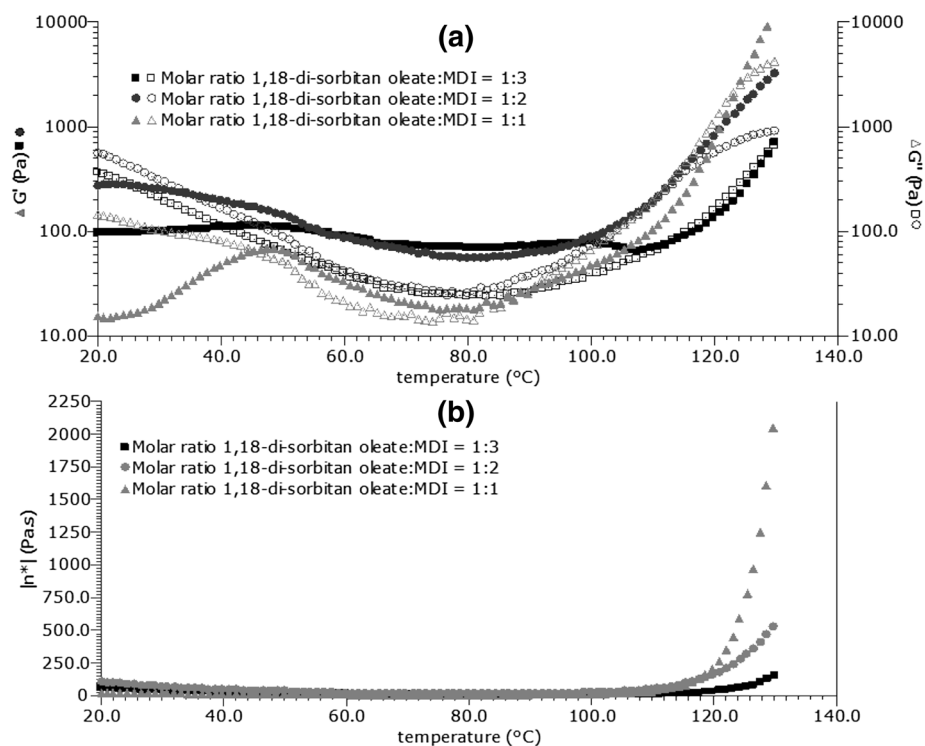


Fig. 7 Theoretical polyurethane structure formed by 1,18-di-sorbitan oleate and MDI

**Fig. 8** Thermo-rheological curves of reaction between 1,18-di-sorbitan oleate and MDI with different molar ratio



**Fig. 9** Viscosity behavior during curing process for different aliphatic diols

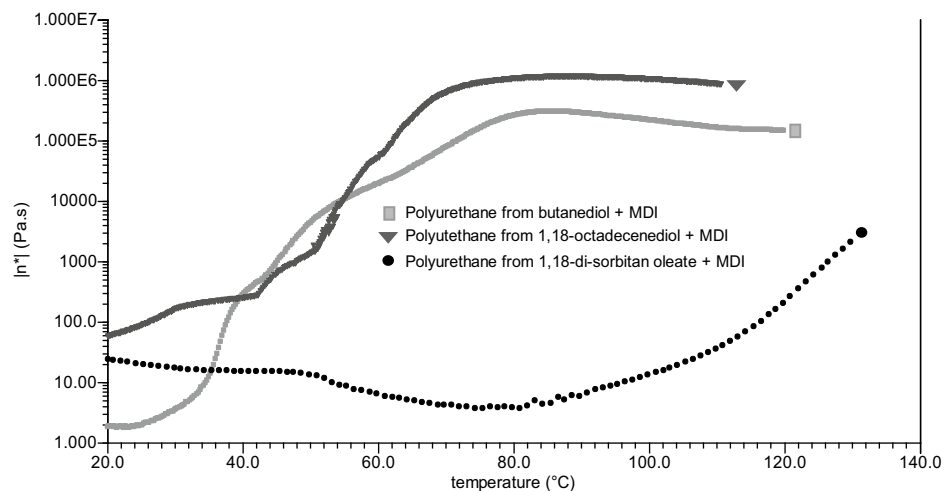
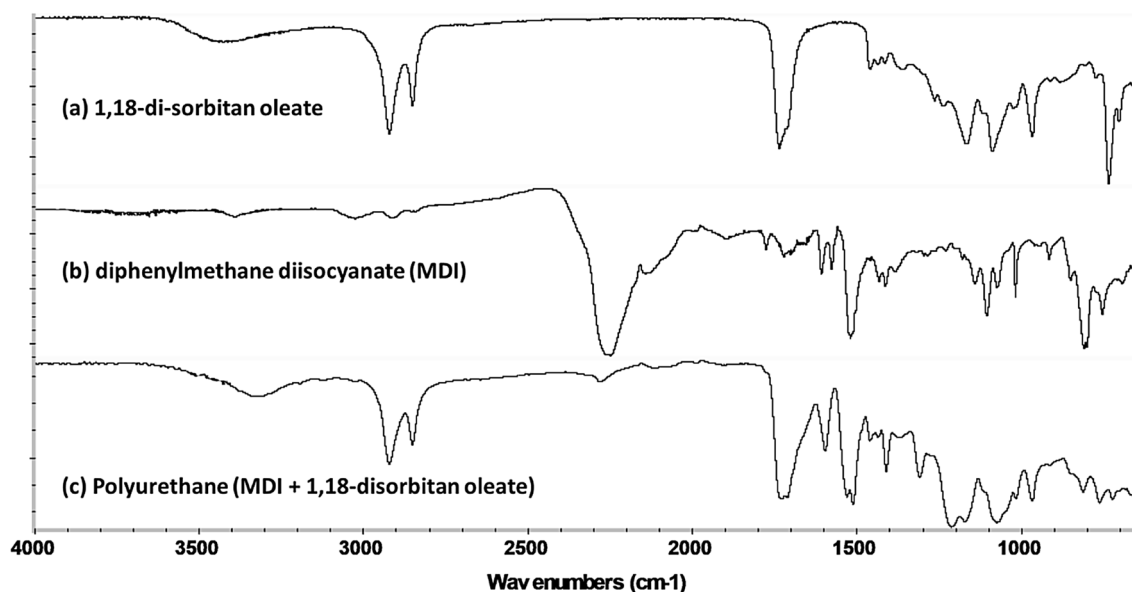


Fig. 9 the 1,18 disorbitan oleate/MDI reaction is included (●). Moreover, it can be observed that a short-chain diol as butenediol causes a shift of polymerization initiation to lower temperature nearly 35 °C and displays a viscosity plateau at 80 °C, whereas large-chain diol as oleic diol starts polymerization above melting temperature around 50 °C and exhibits a viscosity plateau at 70 °C. Finally, di-sorbitan oleate/MDI reaction starts above 100 °C but viscosity plateau is unreached in the observed temperature range up to 130 °C. This reaction behavior may be explained to the lesser reactivity of hydroxy group in sorbitan compared to that for either oleic diol or butenediol. Therefore, synthesis

of polyurethanes by using di-sorbitan oleate monomer is feasible.

ATR–FTIR technique was employed to confirm polyurethane formation from di-sorbitan oleate monomer by using specific polyurethane films. Those films were obtained by thermo-compression process at 130 °C with a clamping force of 1.0 Ton for 30 min to guarantee complete cured state in the reaction product.

The synthesized PU was analyzed by ATR-FTIR to confirm the formation of urethane groups. Figure 10 shows ATR-FTIR spectra for (a) 1,18-di-sorbitan oleate (b) diphenylmethane diisocyanate (MDI) and (c) polyurethane



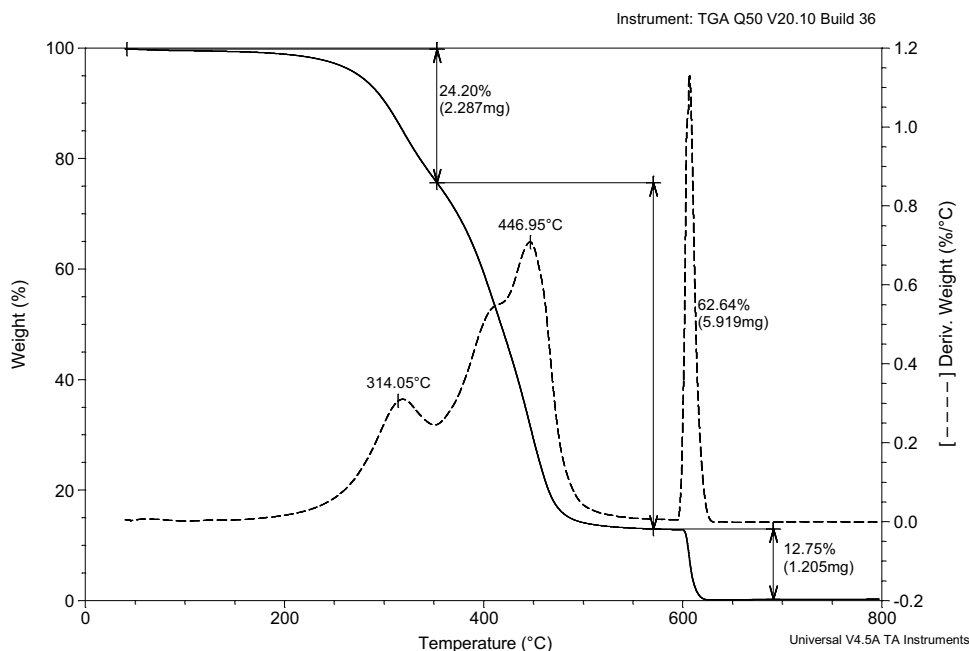
**Fig. 10** Comparison of FTIR spectrum of **a** 1,18-di-sorbitan oleate **b** diphenylmethane diisocyanate (MDI) and **c** polyurethane produced by reaction between MDI and 1,18-di-sorbitan oleate

produced by MDI and 1,18-di-sorbitan oleate reaction. The PU spectrum (Fig. 10c) presents the characteristic bands: stretching of carbonyl of carbamate (NCOO) at  $1711\text{ cm}^{-1}$ , deformation vibration of N–H at  $1596\text{ cm}^{-1}$ , asymmetric stretching of C–O–C at  $1215\text{ cm}^{-1}$  and symmetric stretching of C–O–C at  $1074\text{ cm}^{-1}$ . Between  $3200$  to  $3600\text{ cm}^{-1}$  can be observed a signal attributed to both stretching of O–H and N–H; this is due to the formation of urethane groups and the remaining –OH of the sorbitan as can be observed too in monomer spectrum in Fig. 10b. Other signals corresponding

to sorbitan oleate are observed in the PU spectrum, as alkyl C–H stretching at  $2850$ – $2950\text{ cm}^{-1}$ , –trans double bond at  $965\text{ cm}^{-1}$  and carbonyl ester at  $1736\text{ cm}^{-1}$ . While representative isocyanate vibration at  $2200\text{ cm}^{-1}$  is observed in the MDI spectrum, in the polyurethane spectrum practically disappears. This suggests that most of MDI react with the sorbitan oleate monomer and there are remaining hydroxy groups.

The typical two-steps decomposition of polyurethane [51] was observed by thermogravimetric analysis (TGA) from

**Fig. 11** Thermogravimetric analysis of polyurethane produced by MDI and 1,18-di-sorbitan oleate reaction



room temperature to 580 °C, as seen in the thermal diagram in Fig. 11. The first decomposition process is located at 314 °C that includes depolymerization process with the formation of primary amines, carbon dioxide and polyethylene glycol, it means, thermal degradation of urethane and urea groups, and the second one at 447 °C with a clear shoulder at 400 °C corresponding to both formation of amines and thermal degradation of polyethylene glycol oligomers [52].

It is important to highlight that this second decomposition peak has a shoulder at lower temperature that can be associated to decomposition of sorbitan group. Mass weight loss of the first decomposition was 24%, whereas mass loss for the second peak was close to 63%. This mass percentage agreed with the mass composition of the PU formed by MDI and 1,18-di-sorbitan oleate. At last, it can be observed that this bio-based PU is thermally stable up to 200 °C.

A comparative of TGA curves corresponding to some PU obtained with various diols is shown in Fig. 12. PU obtained from a short diol as butenediol show decomposition peaks at more moderate temperatures compared to oleic diol and di-sorbitan oleate monomers. It can be observed that some differences in decomposition temperatures can be associated to chemical structure. PU obtained from di-sorbitan oleate monomer (long and more voluminous monomeric unit) has more elevated decomposition temperatures compared with PU obtained with butenediol (shorter monomeric unit), but PU obtained from oleyl diol (long monomeric unit) shown the highest decomposition temperatures.

Dynamical-mechanical analysis (DMA) of a thermo-compressed sample of the partially bio-based PU obtained from 1,18-di-sorbitan oleate and MDI was carried out to determine viscoelastic properties of the polymer. Storage modulus ( $G'$ ) and  $\tan \delta$  behavior as function of temperature is shown in Fig. 13. It can be observed that  $G'$  shows a first plateau region at 605 MPa below the glass transition region corresponding to the glassy state modulus  $G_g$ . Additionally, it is observed a shoulder in the  $\tan \delta$  behavior as function of temperature at around 0 °C, which may be attributed to a weak signal of its glass transition temperature ( $T_g$ ), and a well-defined  $\tan \delta$  peak with a maximum at 76 °C. This last peak can be attributed to the melting process of the crystalline domains in the polyurethane. Therefore, the maximum of  $\tan \delta$  peak can be assigned as its melting temperature ( $T_m$ ). As seen in Fig. 13, these transitions detected by DMA are confirmed through differential scanning calorimetry analysis (DSC), where the glass transition temperature ( $T_g$ ) is located near 0 °C and the melting temperature ( $T_m$ ) at around 90 °C. This transition is observed as a broad endothermic process with a melting enthalpy of 36 J/g. Also, in Fig. 13 can be observed that  $G'$  at room temperature decreases to 403 MPa, but between 40 °C and 110 °C, the elastic behavior ( $G'$ ) of the sorbitan oleate-based PU is highly sensitive to temperature changes due to the observed broad transition attributed to its crystalline re-arrangements and melting process. Above 110 °C, the polyurethane shows a second  $G'$  plateau may be attributed to a weak network structure before the flow region.

**Fig. 12** Derivative weight curves of some PU obtained with various diols reacting with MDI (molar ratio 1:1): 1,18-di-sorbitan oleate, 1,18 octadecenediol and butenediol

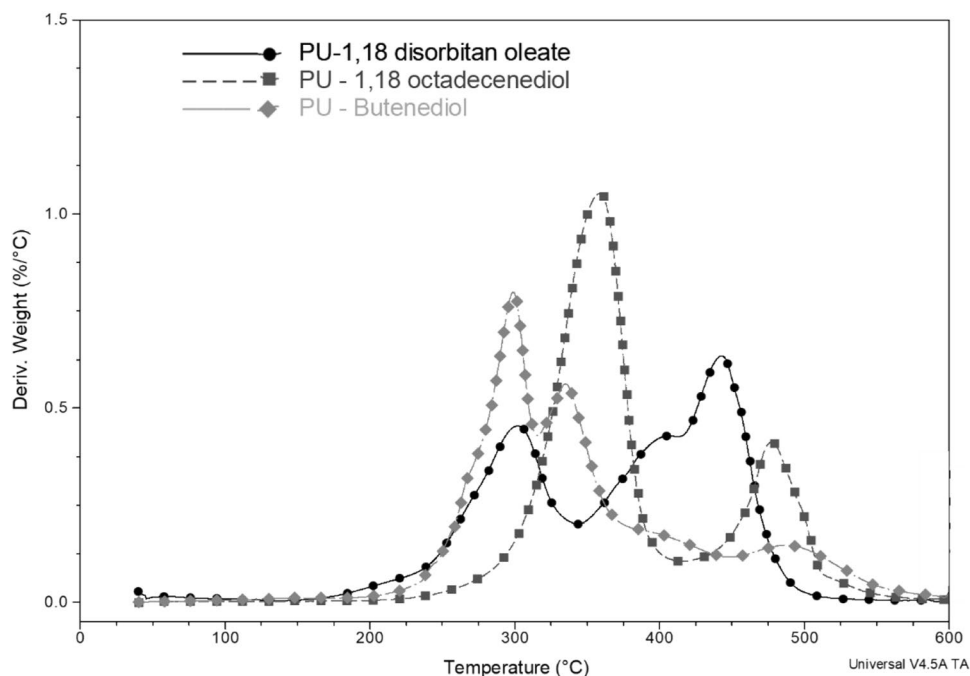
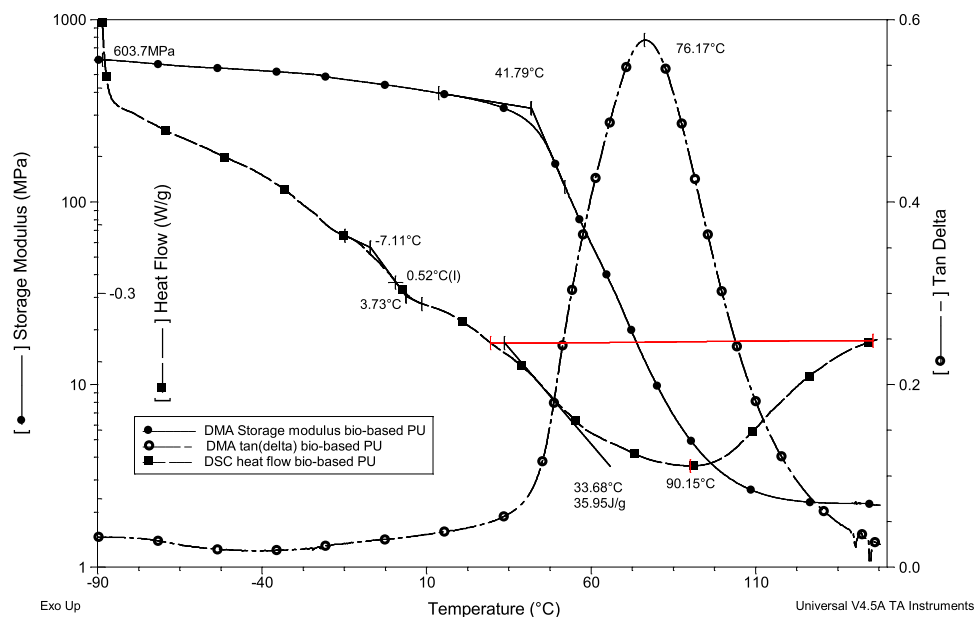


**Fig. 13** Dynamical-mechanical analysis (DMA) and differential scanning calorimetry (DSC) curves of bio-based PU obtained from 1,18-di-sorbitan oleate and MDI



## Conclusions

A chain-end functional di-sorbitan oleate monomer was synthesized through a proposed three-step process. 1,18-octadec-9-enedioic acid was produced through a cross metathesis reaction of oleic acid. After that, a chlorination reaction of this last compound was carried out to obtain 1,18-octadec-enoyl-dichloride. Finally, this compound was esterified with the product of sorbitol dehydration, which was mostly 1,4-sorbitan, to get the functional monomer. A process comprising size exclusion chromatography and column chromatography was used to purify the di-sorbitan oleate monomer. Both  $^1\text{H-NMR}$  and FTIR techniques allowed to confirm that most of the synthesized and purified monomer contains the structure of oleic chains with terminal sorbitan groups. However, with the current data, it cannot be discarded the presence of other compounds obtained by remnant sorbitol, isomers or by side reactions with secondary alcohols during esterification with 1,4-sorbitan. It is necessary to deep about the structure of the compound through complementary analytical techniques, such as MS or  $^{13}\text{C-NMR}$ .

$G'$ ,  $G''$  and  $\tan$  curves as a function of temperature were used to establish the gel point at 110 °C as the starting polymerization reaction to yield bio-based polyurethanes. Furthermore, the polymerization reaction, between the obtained sorbitan end-chain functional monomer and MDI, was confirmed by using the complex viscosity ( $\eta^*$ ) as a function of temperature because of the significant increase on  $\eta^*$  above 100 °C.

According to FTIR results, it was possible to observe the presence of both O–H and N–H groups between 3200 and 3600  $\text{cm}^{-1}$ . Therefore, the hydroxy groups in the sorbitan

oleate monomer can react with isocyanates to yield urethane groups forming the bio-based polyurethane.

The sorbitan oleate-based PU shows a  $T_g$  near 0 °C, a  $T_m$  of 76 °C and a  $G'$  of 400 MPa at room temperature. Between 40 °C and 110 °C, the elastic component ( $G'$ ) of the bio-based PU is very sensitive to temperature changes due to the broad melting process observed, and above 110 °C, the effect of a weak network structure forms a second  $G'$  plateau. Thermal decomposition of the bio-based PU exhibits a typical behavior showing two decomposition peaks, the first peak at 314 °C is associated to degradation of urethane groups through formation of primary amines, carbon dioxide and polyethylene glycol, and the second peak is associated to formation of amines and thermal degradation of polyethylene glycol oligomers.

**Acknowledgements** The authors wish to thank the National Council of Science and Technology of Mexico (CONACYT) for supporting this research work through the project CB-2015–01-257591.

## References

- Mülhaupt R (2013) *Macromol Chem Phys* 214:159
- Budzianowski WM (2017) *Renew Sustain Energy Rev* 70:793
- Sheldon RA (2016) *J Mol Catal A: Chem* 422:3
- Wang J et al (2017) *Waste Manage* 65:11
- John G et al (2019) *Prog Polym Sci* 92:158
- Zhang C et al (2017) *Prog Polym Sci* 71:91
- Gandini A, Lacerda TM (2015) *Prog Polym Sci* 48:1
- Salimon J, Salih N, Yousif E (2012) *Arab J Chem* 5(2):135
- Yabushita M, Kobayashi H, Fukuoka A (2014) *Appl Catal B* 145:1
- Rose M, Palkovits R (2012) *Chemsuschem* 5(1):167
- Rusu OA et al (2015) *Appl Catal B* 176–177:139
- Cao D et al (2016) *Appl Catal A* 528:59
- Ginés-Molina MJ et al (2017) *Appl Catal A* 537:66

14. Cubo A et al (2017) *Appl Catal A* 531:151
15. Zhang Y et al (2018) *Mol Catal* 458:19
16. Dussette C et al (2019) *Mol Catal* 463:61
17. Yuan D et al (2019) *Appl Catal B* 240:182
18. Gustini L et al (2015) *Eur Polymer J* 67:459
19. Bersot JC et al (2011) *Macromol Chem Phys* 212(19):2114
20. Brack, H., et al. (2011) US 2011/0077377A1 SABIC Innov Plast IP BV.
21. Jeong G-T et al (2007) *Appl Biochem Biotechnol* 137(1):935
22. Ng SH et al (2013) *J Nanobiotechnol* 11(1):27
23. Ciriminna R et al (2014) *Sustain Chem Process* 2(1):26
24. Hojabri L, Kong X, Narine S (2010) *J Polym Sci A: Polym Chem* 48(15):3302
25. More AS et al (2013) *Eur Polymer J* 49(4):823
26. Charlon M et al (2014) *Eur Polymer J* 61:197
27. del Río E et al (2011) *Macromol Chem Phys* 212(13):1392
28. Miao S et al (2012) *Eur J Lipid Sci Technol* 114(12):1345
29. Kalita H, Karak N (2014) *J Appl Polym Sci* 131(1):39579
30. Fourati Y et al (2017) *Prog Org Coat* 105:48
31. Mol J (1994) *J Mol Catal* 90(1–2):185
32. Mol J, Khosravi E, SzymanskaBuzar T (2002) *Ring Open Metathesis Polym Relat Chem* 56:377
33. Mol J (2004) *Top Catal* 27(1–4):97
34. Mol JC (2004) *J Mol Catal A: Chem* 213(1):39
35. Ngo H, Jones K, Foglia T (2006) *J Am Oil Chem Soc* 83(7):629
36. Ngo H, Foglia T (2007) *J Am Oil Chem Soc* 84(8):777
37. Zerkowski J, Solaiman D (2012) *J Am Oil Chem Soc* 89(7):1325
38. Kadyrov R et al (2012) *Top Catal* 55(7–10):538
39. Vyshnavi Y, Prasad RBN, Karuna MSL (2013) *Ind Crops Prod* 50:701
40. Aguilar-Castro C et al (2019) *J Appl Polym Sci* 136(8):47095
41. Yabushita, M. (2016) in a study on catalytic conversion of non-food biomass into chemicals: fusion of chemical sciences and engineering, Springer, Editor p.127
42. Yabushita M et al (2015) *Bull Chem Soc Jpn* 88(7):996
43. Petrović ZS et al (2010) *Eur J Lipid Sci Technol* 112(1):97
44. Miao S et al (2014) *Acta Biomater* 10:1692
45. Riyapan D, Saetung A, Saetung N (2019) *J Polym Environ* 27:1693
46. Dhaliwal GS, Anandan S, Chandrashekhara K et al (2019) *J Polym Environ* 27:1897
47. Bresolin D, Valério A, de Oliveira D et al (2018) *J Polym Environ* 26:2467
48. Zhuang JM, Steiner Paul R (1993) in *Holzforschung – Int J Biol. Chem, Phys Technol Wood* p, p 425
49. Yang PF, Han YD, Li TD (2011) *Adv Mater Res* 150–151:23
50. Lu M-Y et al (2018) *Croat Chem Acta* 91(3):299
51. Krämer RH et al (2010) *Polym Degrad Stab* 95(6):1115
52. Ketata N et al (2005) *Polym Polym Compos* 13(1):1

**Publisher's Note** Springer Nature remains neutral with regard to jurisdictional claims in published maps and institutional affiliations.